NASA/TM—2008-215059

Investigating Dielectric and Metamaterial Effects in a Terahertz Traveling-Wave Tube Amplifier

David P. Starinshak
Ohio Aerospace Institute, Brook Park, Ohio

Jeffrey D. Wilson
Glenn Research Center, Cleveland, Ohio

February 2008

NASA STI Program . . . in Profile

Since its founding, NASA has been dedicated to the advancement of aeronautics and space science. The NASA Scientific and Technical Information (STI) program plays a key part in helping NASA maintain this important role.

The NASA STI Program operates under the auspices of the Agency Chief Information Officer. It collects, organizes, provides for archiving, and disseminates NASA's STI. The NASA STI program provides access to the NASA Aeronautics and Space Database and its public interface, the NASA Technical Reports Server, thus providing one of the largest collections of aeronautical and space science STI in the world. Results are published in both non-NASA channels and by NASA in the NASA STI Report Series, which includes the following report types:

- TECHNICAL PUBLICATION. Reports of completed research or a major significant phase of research that present the results of NASA programs and include extensive data or theoretical analysis. Includes compilations of significant scientific and technical data and information deemed to be of continuing reference value. NASA counterpart of peer-reviewed formal professional papers but has less stringent limitations on manuscript length and extent of graphic presentations.

- TECHNICAL MEMORANDUM. Scientific and technical findings that are preliminary or of specialized interest, e.g., quick release reports, working papers, and bibliographies that contain minimal annotation. Does not contain extensive analysis.

- CONTRACTOR REPORT. Scientific and technical findings by NASA-sponsored contractors and grantees.

- CONFERENCE PUBLICATION. Collected papers from scientific and technical conferences, symposia, seminars, or other meetings sponsored or cosponsored by NASA.

- SPECIAL PUBLICATION. Scientific, technical, or historical information from NASA programs, projects, and missions, often concerned with subjects having substantial public interest.

- TECHNICAL TRANSLATION. English-language translations of foreign scientific and technical material pertinent to NASA's mission.

Specialized services also include creating custom thesauri, building customized databases, organizing and publishing research results.

For more information about the NASA STI program, see the following:

- Access the NASA STI program home page at *http://www.sti.nasa.gov*

- E-mail your question via the Internet to *help@sti.nasa.gov*

- Fax your question to the NASA STI Help Desk at 301–621–0134

- Telephone the NASA STI Help Desk at 301–621–0390

- Write to:
  NASA Center for AeroSpace Information (CASI)
  7115 Standard Drive
  Hanover, MD 21076–1320

NASA/TM—2008-215059

Investigating Dielectric and Metamaterial Effects in a Terahertz Traveling-Wave Tube Amplifier

David P. Starinshak
Ohio Aerospace Institute, Brook Park, Ohio

Jeffrey D. Wilson
Glenn Research Center, Cleveland, Ohio

National Aeronautics and
Space Administration

Glenn Research Center
Cleveland, Ohio 44135

February 2008

Acknowledgments

The authors would like to thank Dr. Carol L. Kory, Christine Chevalier, Karl Vaden, and Ian Nemitz for their valuable insights. This work was supported by the NASA Glenn Research Center's Independent Research and Development fund.

This report contains preliminary findings, subject to revision as analysis proceeds.

Level of Review: This material has been technically reviewed by technical management.

Available from

NASA Center for Aerospace Information
7115 Standard Drive
Hanover, MD 21076–1320

National Technical Information Service
5285 Port Royal Road
Springfield, VA 22161

Available electronically at http://gltrs.grc.nasa.gov

Investigating Dielectric and Metamaterial Effects in a Terahertz Traveling-Wave Tube Amplifier

David P. Starinshak
Ohio Aerospace Institute
Brook Park, Ohio 44142

Jeffrey D. Wilson
National Aeronautics and Space Administration
Glenn Research Center
Cleveland, Ohio 44135

Summary

Adding material enhancements to a terahertz traveling-wave tube amplifier is investigated. Isotropic dielectrics, negative-index metamaterials, and anisotropic crystals are simulated, and plans to increase the efficiency of the device are discussed. Early results indicate that adding dielectric to the curved sections of the serpentine-shaped slow-wave circuit produce optimal changes in the cold-test characteristics of the device and a minimal drop in operating frequency. Additional results suggest that materials with simultaneously small relative permittivities and electrical conductivities are best suited for increasing the efficiency of the device. More research is required on the subject, and recommendations are given to determine the direction.

Introduction

Dielectrics have long been used to enhance the efficiency of waveguides and traveling-wave tube (TWT) amplifiers. The first field theory analysis of a dielectric-loaded helical TWT showed that greater electron beam coupling and higher efficiency were possible if a thin dielectric sheath was added to the inside of the beam tunnel (ref. 1). Additional studies found that an optimal dielectric constant existed for the beam tunnel sheath to better slow the primary mode and further increase electron beam interaction (ref. 2). Further, experiments have been done using ceramic enhancements to eliminate spurious modes in a gyrotron-traveling-wave tube amplifier and improve overall performance (ref. 3). In this paper, we will investigate applying various material enhancements to the waveguide surfaces of a proposed 0.4-THz traveling-wave tube amplifier to reduce circuit attenuation and increase efficiency. In addition to standard dielectrics, we will examine materials believed to display a negative refractive index (ref. 4), including anisotropic photonic crystals (ref. 5) and metamaterials with negative permittivities and permeabilities (refs. 6 to 9).

Figure 1 displays a schematic of the amplifier under investigation. Pictured in blue is the slow-wave circuit, consisting of a serpentine-shaped folded waveguide with a center-mounted, square beam tunnel. It is modeled as a perfect vacuum. The yellow represents the walls of the slow-wave circuit, which are modeled as perfect electric conductors (PEC). In addition, a Cartesian coordinate system is selected such that the y-axis points down the center of the beam tunnel, the x-axis points horizontally across the width of the circuit, and the z-axis points vertically across the height of the circuit. Hereafter, we will refer to the y-, x-, and z-directions as the axial, horizontal, and vertical direction respectively.

Models of the TWT were completed using COMSOL Multiphysics (ref. 10). Analysis was done using the RF Module's 3-D frequency-domain eigenmode solver. In order to efficiently simulate various dielectric parameters, the program's impedance boundary condition was utilized—a boundary effect that models the interaction between a material surface and a volume. In order to properly use this boundary condition, we make the assumption that the electric field will not penetrate deeply into the dielectric we

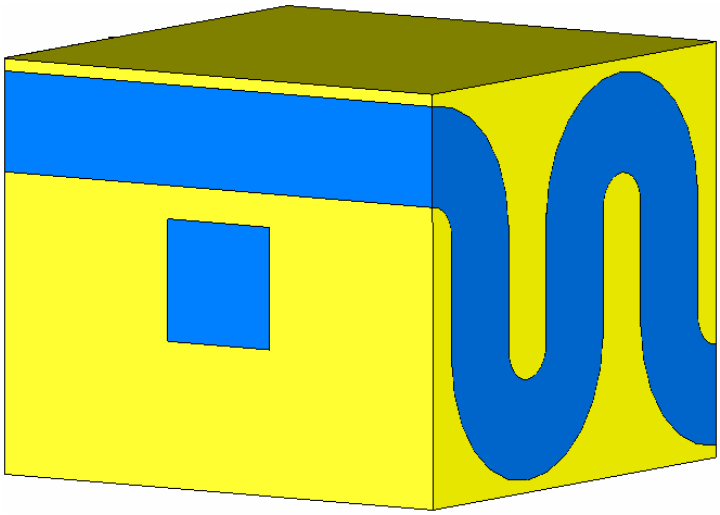

Figure 1.—Serpentine-shaped slow-wave circuit for terahertz traveling-wave tube amplifier. The model has yellow as perfect electric conductor and blue as vacuum.

are modeling. This assumption is valid, considering the small thickness of the dielectric in relation to the width of the folded waveguide.

The power output of a traveling-wave tube amplifier is strongly correlated to its cold-test characteristics, namely on-axis impedance and attenuation. On-axis impedance is a measure of the interaction between the electron beam and the electromagnetic wave inside the circuit. We calculate it for the *n*th space harmonic by

$$K_n = \frac{E_n^2}{2\beta_n^2 P_{RF}} \tag{1}$$

where P_{RF} represents the RF power flow through the circuit (calculated from the axial Poynting vector), β_n the *n*th axial phase constant, and E_n the magnitude of the on-axis electric field for the *n*th harmonic (ref. 11). Likewise, attenuation is a measure of the resistive heating in a given circuit—that is, the power lost per cavity to the conducting walls. Given in decibels per cavity, we calculate circuit attenuation by

$$\alpha = 8.686 \frac{P_L L}{2P_{RF}} \tag{2}$$

where L is the length of a single cavity and P_L is the total power lost per unit length to resistive heating (ref. 12). We assume a conductivity for copper of $\sigma = 5.7\times10^7$ S/m to calculate power loss.

In order to reduce the number of cavities in a TWT amplifier and increase device efficiency, we must maximize the on-axis impedance and minimize attenuation. In order to more easily accomplish this, a single quantity was derived from curve-fitting simulation results with the NASA 2-Dimensional Coupled-Cavity Traveling-Wave Tube Code (ref. 13). It was found that the efficiency for our 0.4 THz TWT slow-wave circuit is proportional to the quantity:

$$\exp\left(0.3231 + 1.251\sqrt{K_n} - 1.532\sqrt{\alpha}\right) \tag{3}$$

Methods to improve the performance of our device will center on optimizing this quantity.

Our approach to increasing efficiency involves changing the boundary conditions inside the folded waveguide by simulating the presence of dielectric on its walls. Adding dielectric blocks the interaction between the electromagnetic wave and the conducting waveguide walls, thus reducing resistive losses and

decreasing attenuation. Furthermore, the orientation of the internal electric and magnetic field vectors change in the vicinity of the dielectric, disrupting the frequency of the simulated standing wave. Decreases in operating frequency, narrowing of bandwidth, and changes to on-axis impedance and efficiency are expected to occur. Our aim is to determine an optimal set of material parameters such that efficiency is maximized and operating frequency is kept high. In addition, we wish to determine a relationship between the cold-test characteristics of our TWT and the relative permeability and permittivity of our simulated dielectrics.

Materials

Three materials were investigated to increase the efficiency of our device: (1) the common dielectric silicon, with relative permittivity $\varepsilon_r = 12.1$, relative permeability $\mu_r = 1$, and electrical conductivity $\sigma = 10^{-12}$ S/m; (2) a general isotropic material with variable permittivity and permeability; and (3) a general anisotropic material with a variable permittivity tensor and $\mu_r = 1$. First, silicon was singled out because of its low conductivity and wide availability. It has found uses in vacuum electronics, waveguides, and traveling-wave tubes for decades, and its capabilities are well-understood. For those reasons, silicon represents an excellent starting point for our investigations.

The second dielectric examined is a general isotropic material. This category includes most normal dielectrics—where the relative permittivity is positive and the relative permeability is unity—as well as negative-index metamaterials (NIMs)—where both permittivity and permeability are simultaneously negative. It should be pointed out that findings involving materials with negative material characteristics and non-unity permeabilities are largely theoretical results. In the case of metamaterials, which oftentimes consist of patterned or repeating geometries of both dielectrics and conductors, their macroscopic material parameters are not well-defined. In addition, the effect they have on incident electromagnetic waves is frequency-dependent. No such metamaterial to date has been constructed to operate at 0.4 THz, and few function over frequency bands wider than 2 to 3 GHz. Thus, present technology is poorly suited for our hypothetical amplifier. However, research is ongoing in the field of metamaterials. Dielectrics with tunable permittivities and permeabilities have been proposed, and work is underway to extend metamaterial properties to higher gigahertz frequencies. Consequently, as metamaterial technology matures, it may prove invaluable in the development of higher-power amplifiers and other vacuum electronics.

The final material under investigation is a general anisotropic crystal. Commonly referred to as photonic crystals, they are periodic, latticed structures that have direction-dependent dielectric constants. Thus, an incident electromagnetic wave will experience different material properties depending on the direction and angle from which it enters the crystal. This property can be expressed mathematically by replacing each material constant with a rank 2 (two array indices are required to describe quantities) material tensor. For the sake of simplicity, we only consider anisotropies in the relative permittivity, with relative permeability set to unity. Moreover, we assume crystals that are oriented along a rectangular coordinate system. This zeroes out all permittivity values except those in the *x*-, *y*-, and *z*-directions, allowing us to express our tensor as

$$\varepsilon = \begin{pmatrix} \varepsilon_{xx} & 0 & 0 \\ 0 & \varepsilon_{yy} & 0 \\ 0 & 0 & \varepsilon_{zz} \end{pmatrix} \tag{4}$$

By varying each of the permittivity components, a direction-dependent relationship can be found between the cold-test characteristics of our TWT and the material properties of our anisotropic dielectric.

It is important to note that electrical conductivity has been removed from our discussion on isotropic and anisotropic materials. Instead, we assume a conductivity of silicon ($\sigma = 10^{-12}$ S/m) for all simulated material. We do this to ensure negligible dielectric losses from our material enhancements as well as to isolate the effects of permittivity and permeability on the cold-test characteristics. In the case of photonic

crystals, this could be argued as a valid assumption, given their uses in low-loss filtering and waveguiding (ref. 5). However, it becomes problematic when we apply this assumption to metamaterials. As mentioned above, their macroscopic material properties are not easily defined. In addition, since most metamaterials are composed of a dielectric base containing a repeating conductive geometry, they suffer from both resistive and absorptive losses (ref. 8). Further, Dewar calculated an effective conductivity of $\sigma_{eff} = 773$ S/m for a metamaterial consisting of a ferrimagnetic dielectric with an array of conducting wires (ref. 9). Therefore, assuming a low conductivity is not valid for current metamaterials. We retain the assumption for these simulations only to isolate the effects of permittivity and permeability.

Methodology and Results

Initial investigations involved using COMSOL's impedance boundary condition to simulate silicon ($\varepsilon_r = 12.1$, $\mu_r = 1$, $\sigma = 10^{-12}$ S/m) on various waveguide walls. Pictures were taken of the surface currents on each of the conducting boundaries and compared to the base model (fig. 2). In addition, dielectric losses, conductive losses, and attenuation were calculated to quantify the effects of adding silicon to various surfaces. Overall, our aim was to minimize attenuation by determining which walls would benefit most from the addition of dielectric. In the end, we found that placing silicon on the curved surfaces of the waveguide produced the largest drop in attenuation.

These results are consistent with previous studies, which found conductive losses to be greatest along the inner curves of the serpentine waveguide (ref. 14). The reason for this is that the orientation of the internal magnetic field vectors—which lie tangent to the waveguide walls—change most rapidly in the vicinity of the inner curves. This rapid change produces substantial current densities, leading to greater

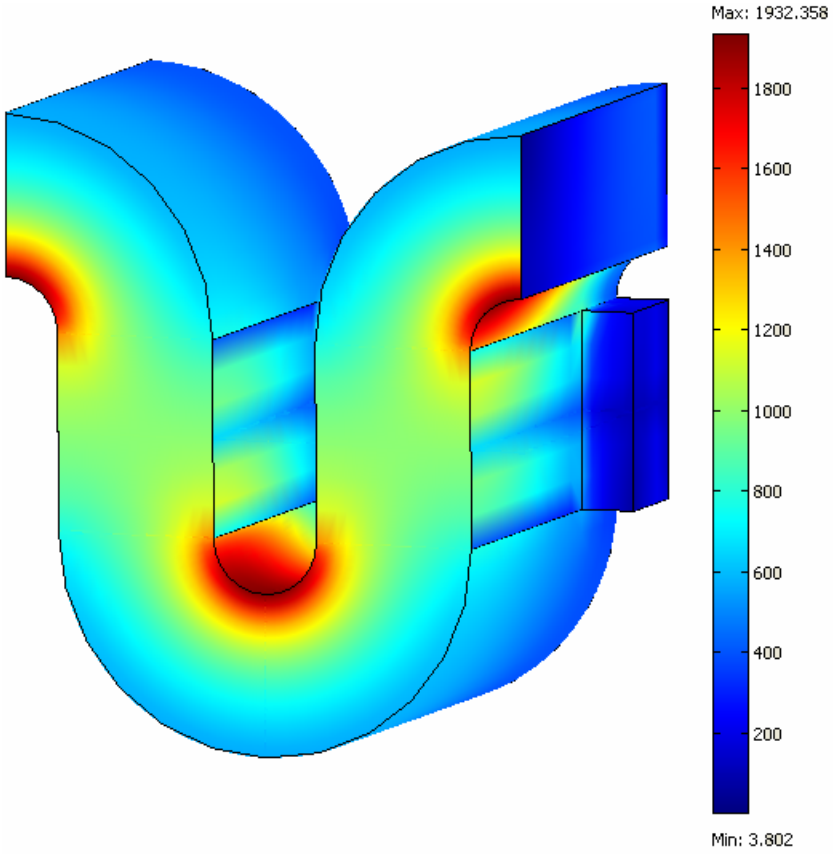

Figure 2.—Half of the slow-wave circuit is modeled. Contours represent surface current densities on the conducting waveguide walls. Note that density is largest along the inside curves.

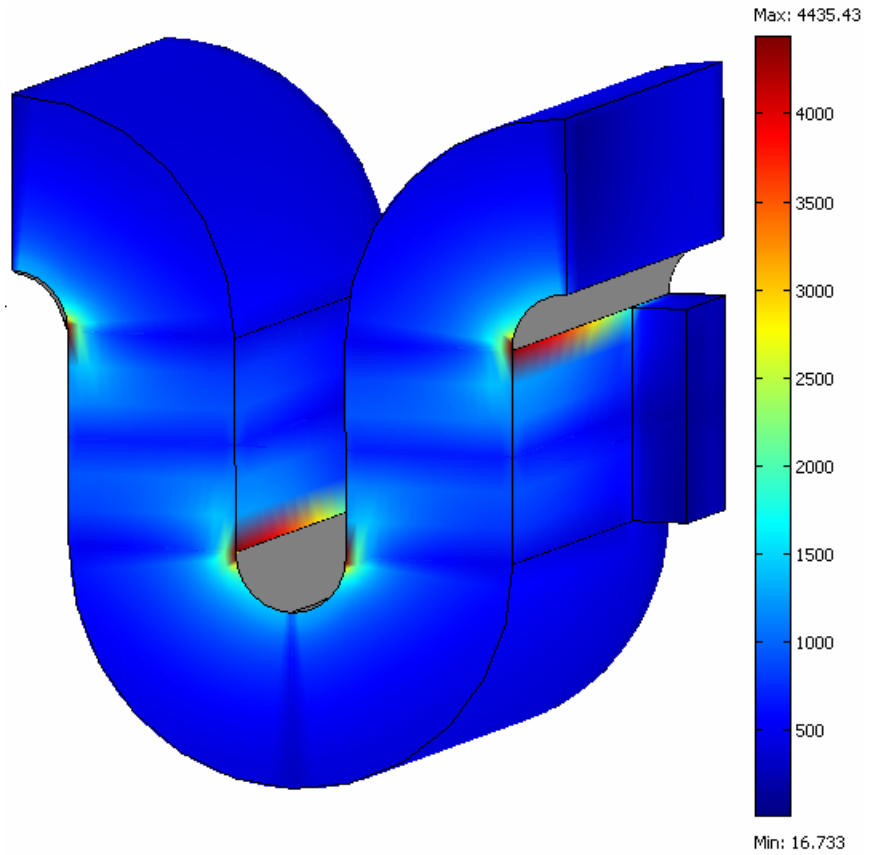

Figure 3.—Half of the slow-wave circuit is modeled, with dark gray areas representing silicon boundaries. Contours are surface current densities. Largest densities appear near the inner curves of the waveguide at the interface between the silicon and the conductors. Magnitudes are larger than in figure 2.

conductive losses in the circuit. Unfortunately, adding dielectric to the waveguide curves is not a perfect solution. The presence of a non-conducting material disrupts the electric and magnetic fields near the waveguide curves, causing surface currents to build up and intensify at the interface between the dielectric and the conducting waveguide walls (fig. 3). Ohmic losses are reduced on average with the addition of silicon, but this is mainly because fewer conducting walls are present to leach power from the internal wave.

In addition to silicon, we tested to see how negative-index metamaterials (NIMs) would affect the cold-test characteristics of our TWT. Three simulations were conducted to test both silicon and an arbitrary NIM with relative permittivity $\varepsilon_r = -1$, relative permeability $\mu_r = -1$, and conductivity $\sigma = 10^{-12}$ S/m. Two of the runs involved placing the materials on the inner curves of the serpentine waveguide, while the other involved only silicon on the outer curves. Eigenfrequencies, impedances, and attenuations were calculated for each, in addition to the relative efficiency calculated from (3). Figure 4 compares the values of each simulation to the cold-test characteristics of the non-enhanced TWT.

As expected, placing dielectric on the inner curves of the waveguide produced the largest drop in attenuation at 0.4 THz. Unfortunately, it also led to huge losses in overall efficiency. For instance, silicon led to an attenuation drop of 45 percent from the original model, with a 60 percent drop in on-axis impedance and more than a 50 percent decrease in efficiency. Likewise, the NIM produced more than a 55 percent drop in attenuation, at the expense of both a 75 percent loss in on-axis impedance and a 65 percent drop in relative efficiency. On the other hand, enhancing the outside curves with silicon did not create as drastic a change. Indeed, the largest drop in operating frequency was only 2 percent across the entire dispersion curve. As a result, attenuation went down by 22 percent, on-axis impedance by

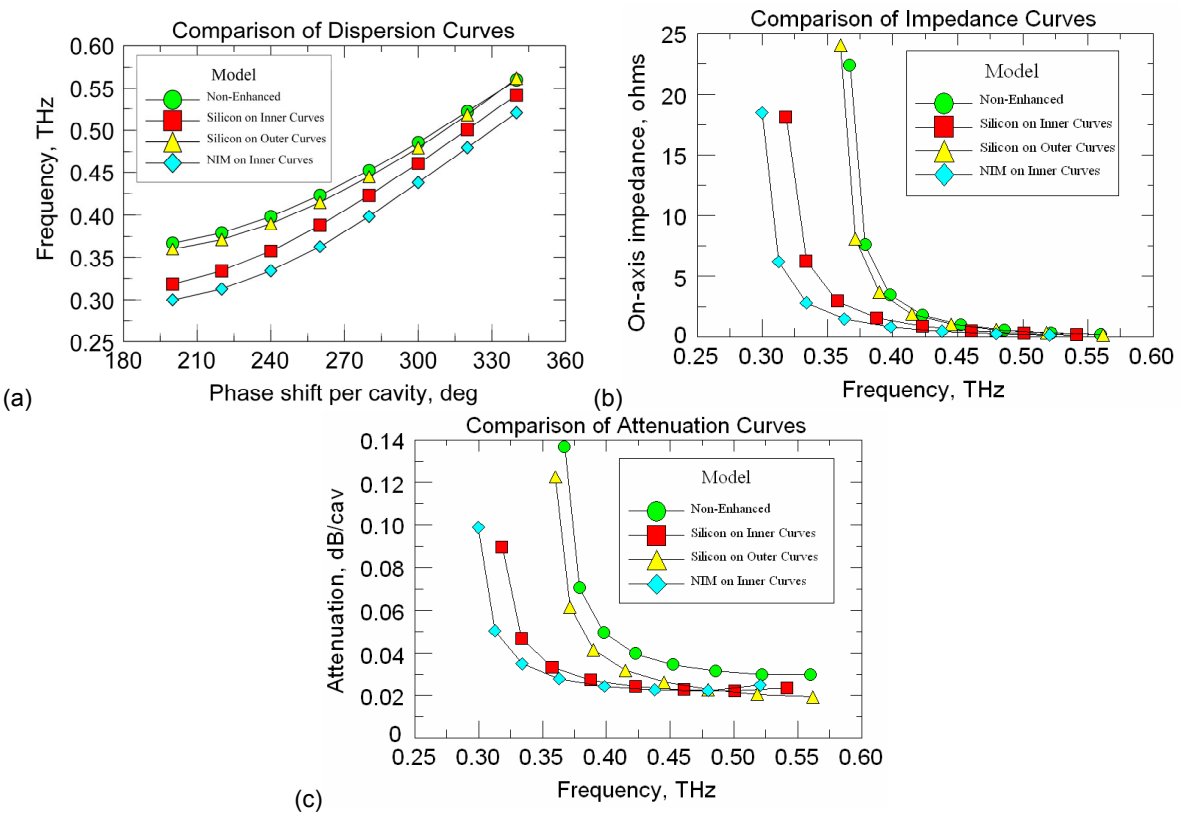

Figure 4.—Cold-test characteristics for the base model compared to those with silicon on the inside waveguide curves, silicon on the outside curves, and negative-index metamaterial on the inside curves. Plots show (a) the dispersion curve, (b) the on-axis impedance, and (c) the attenuation.

11 percent, and relative efficiency by 8 percent. Although these dielectric enhancements do not improve the cold-test characteristics of our TWT with its current dimensions, the results demonstrate that an appreciable drop in attenuation is possible—along with minimal changes to the efficiency of the device—if dielectric is placed only on the outside curves. Moreover, because the drop in operating frequency is small, only a small decrease in the circuit's width will be needed to shift the dispersion curve to a higher operating frequency. Figure 5 illustrates what the slow-wave circuit would look like with material enhancements on the outside curves. As before, the yellow structures are perfect electric conductors and the blue are vacuum; the red is dielectric.

If we consider the fact that the NIM simulation produced the largest changes to the cold-test characteristics, it is conceivable that an optimal relative permittivity and permeability could exist to maximize the efficiency of our device. To test this hypothesis, parameter sweeps were conducted to determine the dependence of the cold-test characteristics on the relative permittivity and relative permeability. In general, it was found that, for a fixed relative permeability and a small electrical conductivity—with permittivity and permeability having opposite signs—both on-axis impedance and attenuation were found to increase as the permittivity approached zero. In addition, the two cold-test characteristics were found to increase at such a rate that the overall efficiency improved for small permittivities. Unfortunately, this result is not particularly realistic. Indeed, for such a material to exist—that is, to have both a small relative permittivity and a small conductivity simultaneously—it would have to absorb very little electric energy like a conductor yet resist the buildup of surface currents like a dielectric. No material in existence is known to display such hybridized properties. However, research in the field of metamaterials may one day produce a periodic structure with these properties.

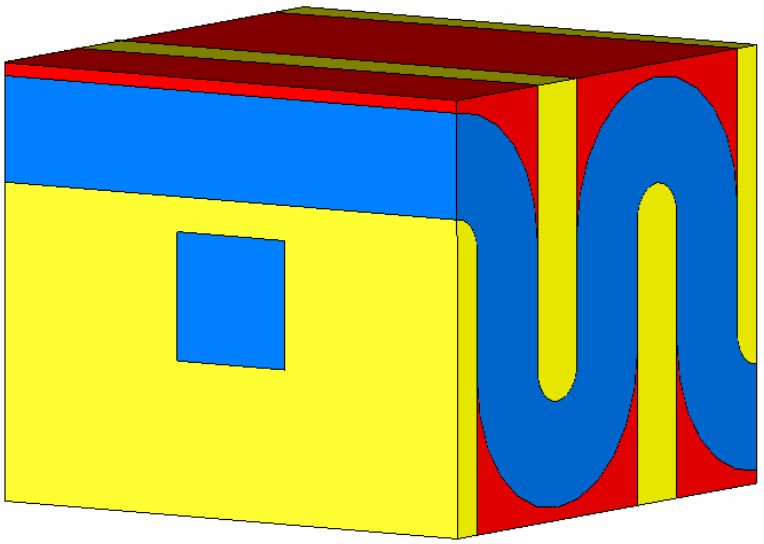

Figure 5.—Serpentine-shaped slow-wave circuit with dielectric enhancements. Yellow areas are modeled as perfect electric conductor, blue as vacuum, and red as dielectric.

In addition to negative-permittivity materials, we experimented with the addition of anisotropic dielectrics. Because of the serpentine shape of our waveguide, most cavity surfaces lay tangent to the horizontal *x*-direction. As a result, we only have significant electric field components along the axial and vertical directions inside the slow-wave circuit and not in the horizontal direction. Since no significant field exists to interact with the horizontal permittivity component, the permittivity tensor of any anisotropic material reduces to only a *y*-component (ε_{yy}) and a *z*-component (ε_{zz}). Thus, all models tested remove the permittivity *x*-component ($\varepsilon_{xx} = 0$) and use $\varepsilon_{yy} \neq \varepsilon_{zz}$. (The case where $\varepsilon_{yy} = \varepsilon_{zz}$ represents a regular isotropic material, which we have already examined.) In addition, we set the relative permeability μ_r to unity and the electrical conductivity σ to 10^{-12} S/m—a valid assumption given the relatively low-loss behavior of many photonic crystals. Both ε_{yy} and ε_{zz} were varied in a parameter sweep over positive and negative values, with operating frequency, on-axis impedance, attenuation, and efficiency calculated for each sweep. Multiphysics optimization algorithms were also run to determine which permittivity tensor produces maximum efficiency.

In general, our anisotropic results are consistent with findings from the isotropic material tests and are similar for each of the following three cases: (1) both ε_{yy} and ε_{zz} positive, (2) both ε_{yy} and ε_{zz} negative, and (3) ε_{yy} positive and ε_{zz} negative. For each case, efficiency was found to increase as each tensor component approached zero. Figure 6 illustrates this trend graphically: 6a for case (1), 6b for case (2), and 6c for case (3). Note also that the largest efficiencies tend to occur when both ε_{yy} and ε_{zz} are simultaneously small and equal. Thus, the optimal permittivity tensor for these three cases is not anisotropic at all. Instead, it confirms the result we found in our isotropic tests—that a dielectric-conductor hybrid with small relative permittivity and small electrical conductivity works best. Finally, scatter plots of efficiency versus frequency (fig. 7) for each case indicate that larger increases in the cold-test characteristics correlate with larger drops in the operating frequency. Consequently, finding an optimal efficiency would be problematic: if we increased efficiency, we would lower our operating frequency, forcing us to rescale our geometry. However, because our geometry has already been optimized for 0.4 THz, rescaling would in turn lower our efficiency. Not only that, we have no guarantee that this new higher efficiency would be any larger of an improvement over the existing model. Therefore, optimizing efficiency at the cost of large drops in operating frequency is not recommended.

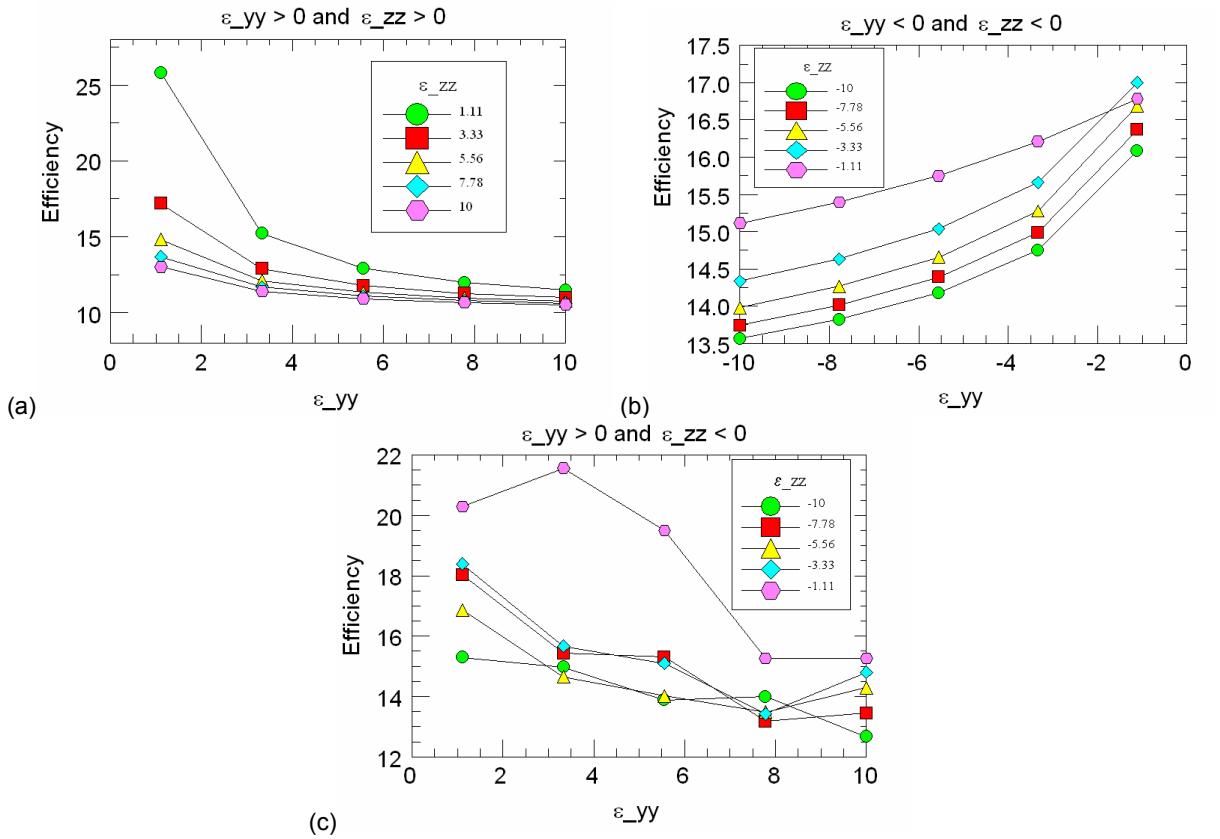

Figure 6.—Device efficiency versus the *y*-component of permittivity for various anisotropic enhancements. The plots are for cases where the *y*- and *z*-components are (a) simultaneously positive, (b) simultaneously negative, and (c) the *y*-component positive and the *z*-component negative.

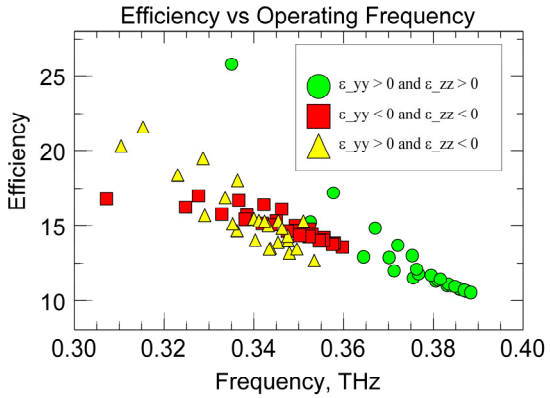

Figure 7.—Device efficiency is plotted against operating frequency for three cases of dielectric with anisotropic permittivity. Note the strong correlation between lower operating frequency and higher efficiency for these three cases.

The fourth case ($\varepsilon_{yy} < 0$ and $\varepsilon_{zz} > 0$) produces slightly different results. The cold-test characteristics are not as frequency-dependent as the other three cases. As the plot in figure 8 illustrates, there is not as strong a correlation between lower operating frequency and higher overall efficiency. Additionally, parameter sweeps were run to find an optimal permittivity tensor. It was determined that a small negative value for ε_{yy} and a value of around 3 for ε_{zz} produce the largest increase in overall efficiency. Figure 9 presents the cold-test characteristics of the enhanced TWT, with ε_{yy} set to –0.0025 and ε_{zz} set to 3.1.

Although the device operates with both a higher efficiency and at a higher frequency than any combination of permittivities in the other three anisotropic cases, the frequency is still low compared to the original model, and substantial rescaling is again required. In addition, the bandwidth has narrowed from 200 GHz to less than 15 GHz—a problem that cannot be fixed by simply scaling the circuit geometry.

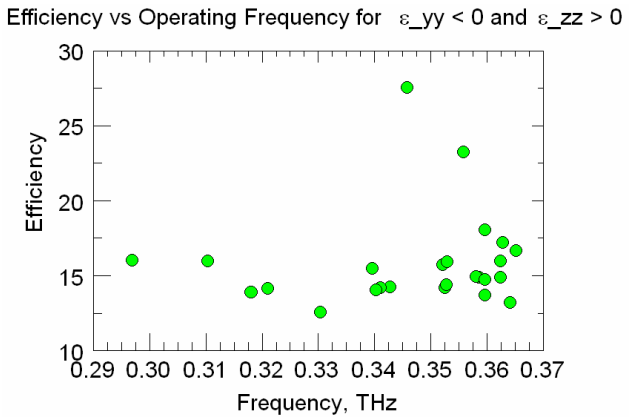

Figure 8.—Device efficiency is plotted against operating frequency for the anisotropic permittivity case of a negative *y*-component and a positive *z*-component. No correlation exists between higher efficiency and lower operating frequency.

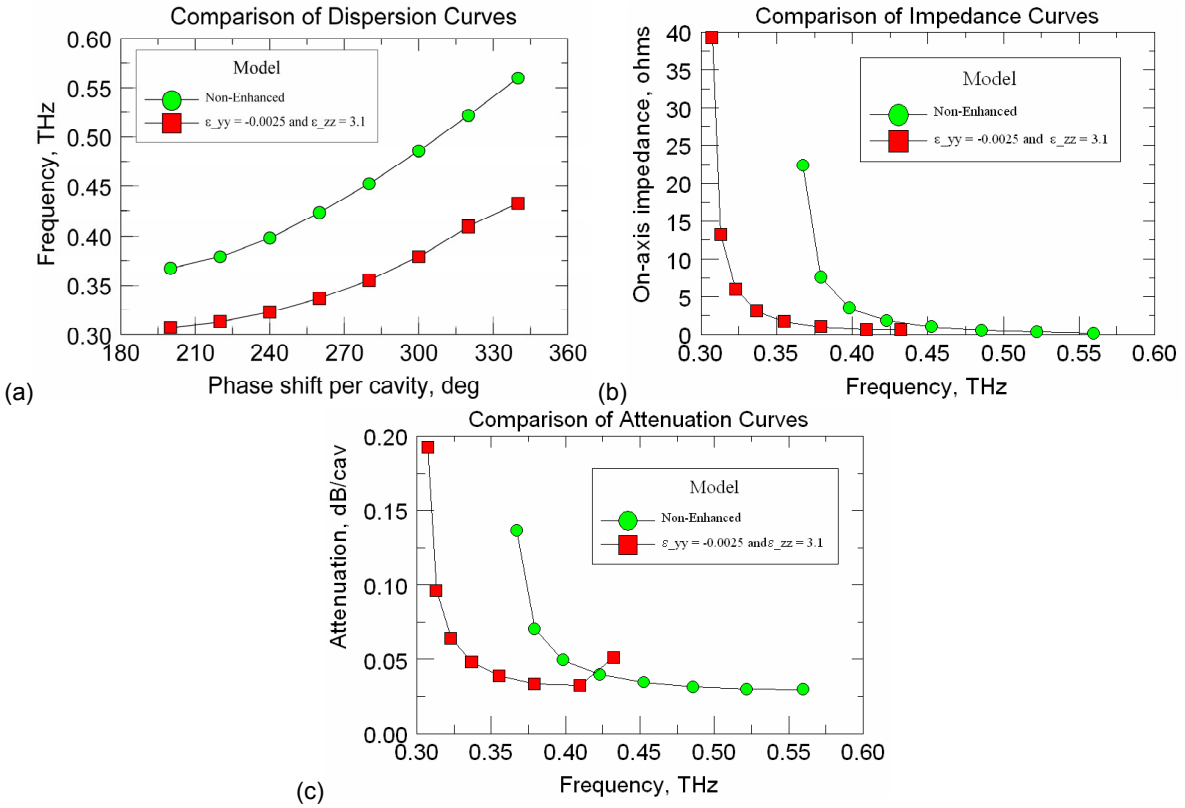

Figure 9.—Cold-test characteristics for an amplifier enhanced with anisotropic-permittivity dielectric. Results are compared to the non-enhanced model in (a) dispersion curve, (b) on-axis impedance, and (c) attenuation.

Conclusions

The incorporation of isotropic, negative-index, and anisotropic dielectrics into designs for a 0.4 THz traveling-wave tube amplifier has been investigated, and an optimal placement location has been found. Assuming a low electrical conductivity, the materials have been found to reduce conductive losses in the circuit. In addition, they have demonstrated sizeable reshaping of the circuit's internal electric and magnetic field vectors, particularly in regions that display large surface current densities. Unfortunately, nearly every dielectric enhancement investigated produced substantial decreases in both operating frequency and bandwidth, indicating that the dimensions of the TWT will need to be rescaled for upcoming simulations. In addition, the materials that demonstrated the greatest efficacy in increasing circuit efficiency are also the least understood and are currently unfeasible to obtain, construct, and incorporate.

With regards to all enhancements modeled, anisotropic crystals were found to work no better than isotropic dielectrics to increase the efficiency of our device. Fabricating an anisotropic crystal to have properly oriented material tensors is a difficult task, especially on small scales. Moreover, simulating anisotropic parameters can lead to the excitation of spurious eigenmodes in finite-element codes, creating additional uncertainty in the model solution. Further, in most of the cases examined, the optimal anisotropic parameters obtained can be approximated by isotropic materials to achieve the same results. Therefore, no additional research can be recommended with regards to anisotropic material enhancements.

Future work in this project will involve testing the dependence of the cold-test characteristics on the electrical conductivity of the material enhancements. Assuming a low conductivity may be valid for low-loss anisotropic structures like photonic crystals, but it produces unrealistic results for materials with small or negative relative permittivities. Silicon was used as a reference for electrical conductivity because of its negligible dielectric losses. Future models, however, will need to include these losses in the calculation of circuit attenuation to get a more complete view of using materials to enhance a traveling-wave tube amplifier.

Now that a methodology is in place to simulate and test material enhancements, as well as trends relating a material's permittivity and permeability to circuit efficiency, additional tests will benefit from taking a more realistic look at existing dielectrics and metamaterials. Overall, as more information becomes available on the macroscopic material characteristics of metamaterials as well as their useful applications in a number of electron devices, a more accurate assessment on the results of this project can be made.

References

1. Freund, H.P.; Zaidman, E.G.; Kodis, M.A.; Vanderplaats, N.R.: Linearized Field Theory of a Dielectric-Loaded Helix Traveling Wave Tube Amplifier. *IEEE Trans. on Plasma Science,* vol. 24, no. 3, 1996.
2. Qian, B.L.; Li, C.L., Liu, Y.G.: Backward- and Traveling-Wave Tubes with Dielectric-Lined Rippled-Wall Waveguides. *Physical Review E*, vol. 53, no. 2, 1996.
3. Garven, M.; Calame, J.P.; Danly, B.G.; Nguyen, K.T.; Levush, B.; Wood, F.N.; Pershing, D.E.: A Gyrotron-Traveling-Wave Tube Amplifier Experiment With a Ceramic Loaded Interaction Region. *IEEE Trans. on Plasma Science*, vol. 30, no. 3, 2002.
4. Veselago, V.G.: The Electrodynamics of Substances with Simultaneously Negative Values of ε and μ. *Soviet Physics Uspekhi*, vol. 10, 1968.
5. Zhang, Y.; Fluegel, B.; Mascarenhas, A.: Total Negative Refraction in Real Crystals for Ballistic Electrons and Light. *Physical Review Letters*, vol. 91, no. 15, 2003.
6. Shelby, R.A.; Smith, D.R.; Schultz, S.: Experimental Verification of Negative Index of Refraction. *Science*, vol. 292, 2001.

7. Chettiar, U.K.; Kildishev, A.V.; Klar, T.A.; Shalaev, V.M.: Negative Index Metamaterial Combining Magnetic Resonators with Metal Films. *Optics Express*, vol. 14, no. 17, 2006.
8. Chettiar, U.K.; Kildishev, A.V.; Klar, T.A.; Yuan, H.-K.; Cai, W.; Sarychev, A.K.; Drachev, V.P., Shalaev, V.M.: From Low-loss to Lossless Optical Negative-Index Materials, CLEO/QELS-06 Annual Meeting Proceedings, Long Beach, CA, May 21-26, 2006.
9. Dewar, G.: A Thin Wire Array and Magnetic Host Structure with n<0. *Journal of Applied Physics*, 2005.
10. COMSOL Multiphysics User's Guide. Version 3.2, COMSOL AB, Sept. 2005.
11. Pierce, John Robinson: Traveling-Wave Tubes. Van Nostrand, New York, NY, 1950.
12. Wilson, J.D. and Kory, C.L.: Simulation of the Cold-Test Parameters and RF Output Power for a Coupled-Cavity Traveling-Wave Tube. *IEEE Trans. Electron Devices*, vol. 442, 1995.
13. Wilson, J.D., "Revised NASA Axially Symmetric Ring Model for Coupled-Cavity Traveling-Wave Tubes," NASA Technical Paper 2675, Jan. 1987.
14. Chevalier, C.T. Personal communication.

REPORT DOCUMENTATION PAGE	Form Approved OMB No. 0704-0188

1. REPORT DATE *(DD-MM-YYYY)*	2. REPORT TYPE	3. DATES COVERED *(From - To)*
01-02-2008	Technical Memorandum	

4. TITLE AND SUBTITLE
Investigating Dielectric and Metamaterial Effects in a Terahertz Traveling-Wave Tube Amplifier

5a. CONTRACT NUMBER

5b. GRANT NUMBER

5c. PROGRAM ELEMENT NUMBER

6. AUTHOR(S)
Starinshak, David, P.; Wilson, Jeffrey, D.

5d. PROJECT NUMBER

5e. TASK NUMBER

5f. WORK UNIT NUMBER
WBS 698671.01.03.45

7. PERFORMING ORGANIZATION NAME(S) AND ADDRESS(ES)
National Aeronautics and Space Administration
John H. Glenn Research Center at Lewis Field
Cleveland, Ohio 44135-3191

8. PERFORMING ORGANIZATION REPORT NUMBER
E-16271

9. SPONSORING/MONITORING AGENCY NAME(S) AND ADDRESS(ES)
National Aeronautics and Space Administration
Washington, DC 20546-0001

10. SPONSORING/MONITORS ACRONYM(S)
NASA

11. SPONSORING/MONITORING REPORT NUMBER
NASA/TM-2008-215059

12. DISTRIBUTION/AVAILABILITY STATEMENT
Unclassified-Unlimited
Subject Category: 33
Available electronically at http://gltrs.grc.nasa.gov
This publication is available from the NASA Center for AeroSpace Information, 301-621-0390

13. SUPPLEMENTARY NOTES

14. ABSTRACT
Adding material enhancements to a terahertz traveling-wave tube amplifier is investigated. Isotropic dielectrics, negative-index metamaterials, and anisotropic crystals are simulated, and plans to increase the efficiency of the device are discussed. Early results indicate that adding dielectric to the curved sections of the serpentine-shaped slow-wave circuit produce optimal changes in the cold-test characteristics of the device and a minimal drop in operating frequency. Additional results suggest that materials with simultaneously small relative permittivities and electrical conductivities are best suited for increasing the efficiency of the device. More research is required on the subject, and recommendations are given to determine the direction.

15. SUBJECT TERMS
Traveling-wave tubes; Electric fields; Dielectrics; Circuits; Permittivity; Permeability

16. SECURITY CLASSIFICATION OF:			17. LIMITATION OF ABSTRACT	18. NUMBER OF PAGES	19a. NAME OF RESPONSIBLE PERSON
a. REPORT	b. ABSTRACT	c. THIS PAGE			STI Help Desk (email:help@sti.nasa.gov)
U	U	U	UU	17	19b. TELEPHONE NUMBER *(include area code)* 301-621-0390